Computational and Structural Biotechnology Journal 23 (2024) 648–658

Contents lists available at ScienceDirect

Computational and Structural Biotechnology Journal

journal homepage: www.elsevier.com/locate/csbj

Research Article

Splicing inhibition mediated by reduced splicing factors and helicases is associated with the cellular response of lung cancer cells to cisplatin

Lujuan Wang [a,c,e,1], Na Yin [c,e,1], Wenhua Shi [c,e], Yaohuan Xie [c,e], Junqi Yi [b,d], Ziying Tang [b,d], Jingqun Tang [b,d,*], Juanjuan Xiang [b,c,e,*]

[a] Hunan Key Laboratory of Tumor Models and Individualized Medicine, The Second Xiangya Hospital, Changsha, Hunan 410011, China
[b] Hunan Key Laboratory of Early Diagnosis and Precise Treatment of Lung Cancer, The Second Xiangya Hospital, Changsha, Hunan 410011, China
[c] Cancer Research Institute, School of Basic Medical Science, Central South University, Changsha, Hunan 410011, China
[d] Department of Thoracic Surgery, The Second Xiangya Hospital, Central South University, Changsha, Hunan 410011, China
[e] NHC Key Laboratory of Carcinogenesis and the Key Laboratory of Carcinogenesis and Cancer Invasion of the Chinese Ministry of Education, Xiangya Hospital, Central South University, Changsha, Hunan 410013, China

ARTICLE INFO

Keywords:
Cell dormancy
Chemotherapy
Lung adenocarcinoma cells
Splicing inhibition

ABSTRACT

Lung cancer's mortality is predominantly linked to post-chemotherapy recurrence, driven by the reactivation of dormant cancer cells. Despite the critical role of these reactivated cells in cancer recurrence and metastasis, the molecular mechanisms governing their therapeutic selection remain poorly understood. In this study, we conducted an integrative analysis by combining PacBio single molecule real-time (SMRT) sequencing with short reads Illumina RNA-seq. Our study revealed that cisplatin-induced dormant and reactivated cancer cells exhibited a noteworthy reduction in gene transcripts and alternative splicing events. Particularly, the differential alternative splicing events were found to be overlapping with the differentially expression genes and enriched in genes related to cell cycle and cell division. Utilizing ENCORI database and correlation analysis, we identified key splicing factors, including SRSF7, SRSF3, PRPF8, and HNRNPC, as well as RNA helicase such as EIF4A3, DDX39A, DDX11, and BRIP1, which were associated with the observed reduction in alternative splicing and subsequent decrease in gene expression. Our study demonstrated that lung cancer cells reduce gene transcripts through diminished alternative splicing events mediated by specific splicing factors and RNA helicase in response to the chemotherapeutic stress. These findings provide insights into the molecular mechanisms underlying the therapeutic selection and reactivation of dormant cancer cells. This discovery opens a potential avenue for the development of therapeutic strategies aimed at preventing cancer recurrence following chemotherapy.

1. Introduction

Lung cancer is one of the most common cancers with high morbidity and mortality rates, categorized into small-cell lung cancers (SCLC) and non-small-cell lung cancers (NSCLC). Standard treatment modalities include surgery, chemotherapy, radiotherapy, targeted therapy, and immunotherapy. Cisplatin (DDP)-based chemotherapy remains the primary approach for NSCLC; however, its efficacy is often compromised by drug resistance, leading to tumor recurrence [1]. Cancer dormancy subsequent to chemotherapy constitutes a major factor contributing to tumor recurrence [2]. Understanding the molecular mechanisms governing cancer dormancy and reactivation is a complex challenge. These processes involve a dynamic interplay of genetic, epigenetic, and microenvironmental factors [3] High-throughput technologies, such as cellular barcoding for clonal dynamics monitoring, have provided valuable insights into tumor recurrence, revealing changes in clonal diversity during tumor regression and recurrence [4].

Alternative splicing, an essential mechanism regulating gene

Abbreviations: SMRT, single molecule real-time; SCLC, small-cell lung cancers; NSCLC, non-small-cell lung cancers; DDP, cisplatin; TGS, Third-generation sequencing; PacBio, Pacific Biosciences; RBPs, RNA-binding proteins; TAPIS pipeline, Transcriptome Analysis Pipeline for Isoform Sequencing; AS, alternative splicing; APA, alternative polyadenylation; DSEs, differential alternative splicing events; DSGs, differentially spliced genes; MXE, mutually exclusive exon; SE, skipped exons; A3SS, alternative 3′ splice sites; A5SS, alternative 5′ splice sites; RI, retained introns.

* Correspondence to: The Second Xiangya Hospital, Changsha, Hunan 410011, China.
E-mail addresses: tangjq@csu.edu.cn (J. Tang), xiangjj@csu.edu.cn (J. Xiang).

[1] These authors contribute equally to this study.

https://doi.org/10.1016/j.csbj.2023.12.039
Received 13 September 2023; Received in revised form 17 December 2023; Accepted 26 December 2023
Available online 28 December 2023

expression and RNA/protein diversity, is influenced by cis-acting elements and trans-acting factors, including splicing enhancers or silencers and RNA-binding proteins (RBPs) [5]. While second-generation sequencing has limitations in elucidating RNA splicing due to short reads [6], third-generation sequencing (TGS) technologies, exemplified by PacBio (Pacific Biosciences) single-molecule real-time (SMRT) sequencing, offer advantages by providing full-length transcripts directly without assembly [7]. Despite SMRT's inability to quantify gene expression levels, this challenge can be addressed using Illumina RNA-seq [8].

RBPs, including splicing factors and RNA helicases, are pivotal in RNA processing and pre-mRNA alternative splicing [9]. Splicing factors, categorized into SR proteins and hnRNPs, bind to specific pre-mRNA sequences, regulating the splicing process. RNA helicases unwind RNA secondary structures, facilitating alternative splicing by overcoming impediments to splicing factor access.

In this study, we combined PacBio sequencing and Illumina RNA-seq to investigate alternative splicing mediated by splicing factors and RNA helicases during cellular dormancy and relapse induced by cisplatin. Comprehensive analysis of differentially expressed and differentially spliced genes revealed a strong association between alternative splicing and the dynamic expression of genes during cancer dormancy and relapse.

2. Materials and methods

2.1. Cell culture and treatment

For the human lung adenocarcinoma cell lines A549 (ATCC, CRM-CCL-185™). Cisplatin (P4394) was purchased from SigmaAldrich (Sigma, MO, USA). A549 were treated with cisplatin (7 ng/μl) for 48 h at 37 °C and 5% CO_2 in a humidified incubator as maintained.

2.2. Cell cycle analysis

After treatment of cells with cisplatin for 48 h, the drug was removed and the culture was continued. At different times of culture, cells were collected, fixed in 70% cold ethanol and washed twice with cold PBS, incubated with PI/RNase solution (C1052, Beyotime, China) for 30 min and then put on the machine of flow cytometer (Cytek, DxP13) to detect. The cell cycle results of the samples were evaluated using automated analysis of the ModFit LT software.

2.3. RNA extraction, RNA-seq

These procedures were performed as previously described [10]. Cells after treatment with cisplatin, with 3 replicates each group, underwent total RNA extraction using Trizol (Invitrogen, Carlsbad, CA, USA) according to manual instruction. Total RNA was then underwent qualification and quantification through a Nano Drop and Agilent 2100 bioanalyzer (Thermo Fisher Scientific, MA, USA). A cDNA library was constructed. Briefly, Oligo(dT)-attached magnetic beads were used to purify long transcripts such as mRNA. Purified mRNA was fragmented into small pieces using fragment buffer at an appropriate temperature. Random hexamer-primed reverse transcription was performed to synthesize double-stranded cDNA. The resulting cDNA fragments were amplified by PCR, and products were purified using Ampure XP Beads, followed by dissolution in EB solution. The product was validated on the Agilent Technologies 2100 bioanalyzer for quality control. The final library was amplified with phi29 to generate DNA nanoball (DNB), each containing more than 300 copies of one molecular. The DNBs were loaded onto the patterned nanoarray, and single-end 50-bases reads were generated on BGIseq500 platform (BGI-Shenzhen, China). Sequencing data underwent filtration with SOAPnuke (v1.5.2) [11] by: (1) Removing reads containing sequencing adapter; (2) Removing reads with a low-quality base ratio (base quality less than or equal to 5) exceeding 20%; (3) Removing reads with an unknown base ('N' base) ratio surpassing 5%. Subsequently, clean reads were obtained and stored in FASTQ format. The clean reads were aligned to the reference genome (Homo_sapiens, GCF_000001405.38_GRCh38.p12) using HISAT2 v2.0.4) [12,13]. Bowtie2 (v2.2.5) [14] was applied to align the clean reads to the reference transcriptome. The expression level of genes were calculated using Expectation Maximization (RSEM) (v1.2.12) [15]. Gene expression levels were normalized as fragments per kilobase of exon model per million mapped reads (FPKM) by RSEM. Differential expression analysis was performed using the DESeq2(v1.4.5) [16]with Q value $\leq$ 0.05. The heatmap of differentially expressed genes with unsupervised clustering was generated using the pheatmap package (v1.0.8) in R software. The heatmap represented expression values (log2 (FPKM + 1) of differentially expressed genes. Following unsupervised clustering, Z-sores were calculated for each row (each gene) by subtracting the mean and dividing by the standard deviation. The final heatmap was plotted after being balanced by the Z-score. KEGG enrichment analysis of annotated differential expressed genes was performed by R package ggplot2. Pathway significance levels were corrected by Q value with a rigorous threshold (Q value $\leq$ 0.05). The raw RNA-seq data were deposited in SRA database, with accession number is SRA PRJNA730205.

2.4. PacBio Iso-sequencing

To perform PacBio Iso-Seq, total RNA was collected from the cells representing the control, dormancy and reactivation groups. Eligible RNAs from each group were uniformly mixed, and 2 g of RNA from each group was used as input material for RNA sample preparation. The SMRTbellTM Template Prep Kit facilitated the generation of SMRTbellTM libraries, involving processes including DNA Damage repair, end-repair, A-tailing and adaptor ligation. Library quality was evaluated using the Agilent Bioanalyzer 2100 system. Finally, primers and enzyme were bound to the SMRT template to form a complete SMRT bell library. The SMRTbellTM libraries were prepared according to the Isoform Sequencing Protocol (Iso-Seq) using the Clontech SMARTer PCR cDNA Synthesis Kit, followed by sequencing on the PacBio Sequel II System. The sequence data underwent processing using the SMRT Analysis software (ISOseq version3.0). Alternative splicing events were analyzed with Astalavista. By comparing all given transcripts, AStalavista [17]detects variations in their splicing structure and identifies all AS events by assigning to each of them an AS code. Alternative polyadenylation events analysis (APA) was carried out using reads aligning to each annotated gene using TAPIS pipeline[16]. Predicted full-length transcript structures were compared to known gene structures using MatchAnnot (1.0) [18], assessing how well the full-length transcripts aligned with the reference genome. Functional annotation information of full-length transcripts was obtained by annotating high-quality full--length transcript sequences with databases (NT, NR, Swissprot, GO, KEGG, KOG/COG). To obtain highly accurate genome assembly and gene expression profiles, we used both Illumina and PacBio RNA-seq data. The reads from Illumina RNA-seq were aligned to de novo transcriptome assemblies generated from PacBio sequencing using Expectation Maximization (RSEM). The pipeline was shown in Supplementary Fig. 1. The accession number is SRA PRJNA793575 in the NCBI Sequence Read Archive (SRA) database.

2.5. Alternative splicing analysis and analysis of differentially spliced genes

Alternative splicing events were analyzed with Astalavista [17]. Astalavista detects variants in its splice structure by comparing all given transcripts and identifies all AS events (exon skipping, intron retention, 5′ splice site substitutions, 3′ splice site substitutions, mutually exclusive exons) by assigning an AS code to each exon. lr2rmats (https://github.com/Xinglab/lr2rmats#local) is based on Snakemake analysis and can

generate new annotation files by optimizing the gene annotation files using triple and second data. The newly generated annotation files can be provided to rMATS [19] for differential variable splicing analysis. Genes with FDR< 0.05 & |IncLevelDifference value| > 5% were considered as DSGs.

2.6. Differential expression analysis and analysis of differentially splicing genes

The two conditions were analyzed for differential expression using EdgeR. Derived p-values were adjusted to control for false discovery rates using the Benjamini and Hochberg methods.

2.7. Splicing factors-target interaction analysis

The splicing factors target genes of cell cycle/cell division-related were selected by ENCORI database (https://rna.sysu.edu.cn/encori/tutorialAPI.php). The correlation analysis between the expression of Splicing factors/helicases with cell cycle/cell division-related genes showing by R package. *P < 0.05, * *P < 0.01.

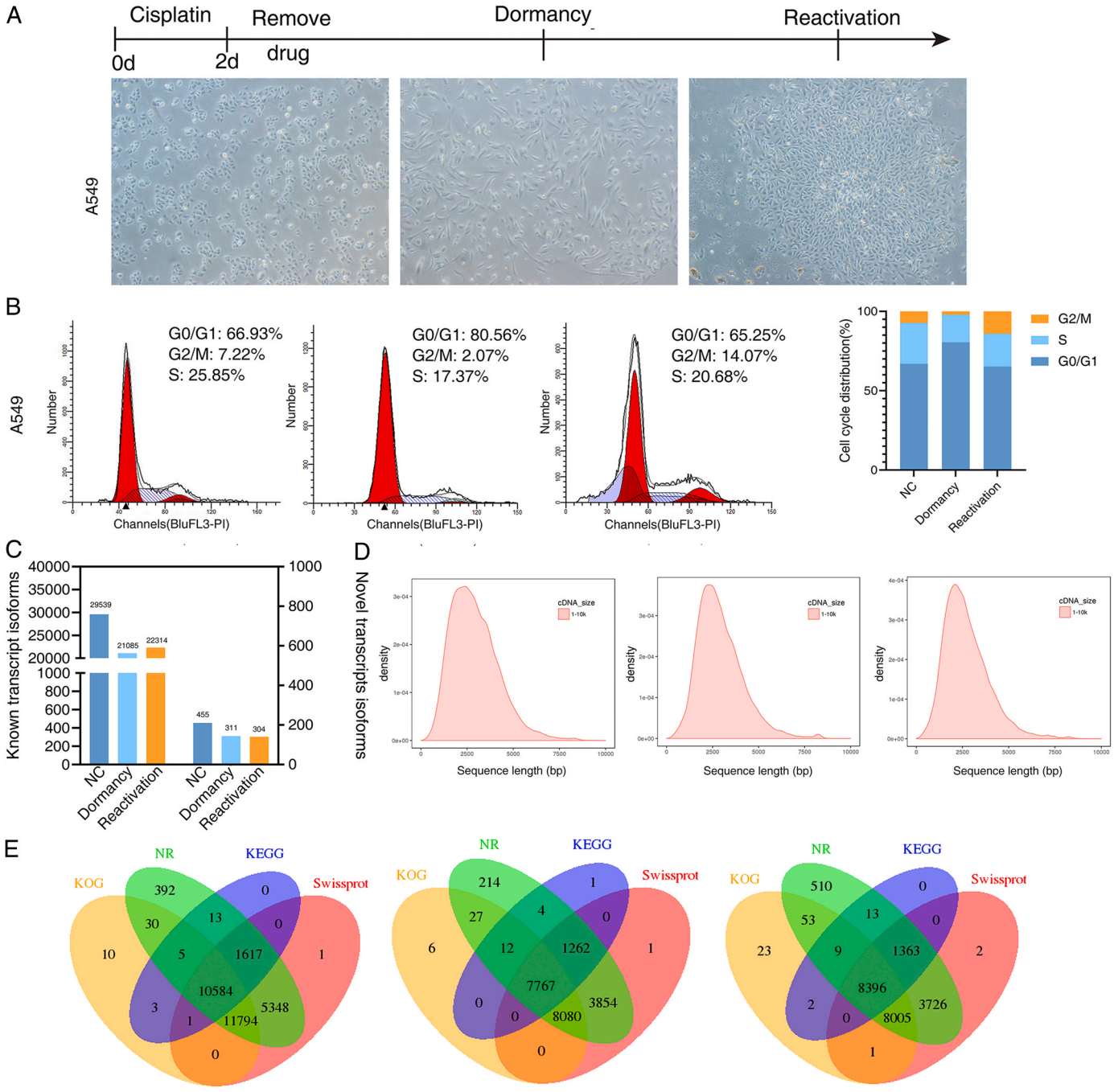

Fig. 1. Chemotherapy-responsive cancer cells exhibited reduced gene transcripts. NSCLC cell lines A549 were treated with cisplatin at 7 ng/μl for 48 hrs, after which the residual cells were cultured for additional days. (A) The images of A549 at different time points during cisplatin treatment. (B) Cell cycle analysis for A549 cells at different time points during cisplatin treatment. (C) All isoforms included known transcript isoforms and novel transcript isoforms in NC, dormant and reactivated cancer cells respectively. (D) The PacBio iso-seq was performed to sequence full-length cDNA. (E) MatchAnnot was employed to compare the transcript isoforms with known transcript isoforms. Student's T test, *P < 0.05, * *P < 0.01, * ** P < 0.001.

3. Results

3.1. Chemotherapy-responsive cancer cells exhibit a reduction in gene transcripts

To investigate the molecular mechanisms governing cellular dormancy and subsequent reactivation post-chemotherapy, we established a cell model emulating reversible tumor dormancy and relapse following cisplatin treatment in lung cancer [20–22]. A549 cells were exposed to cisplatin at a concentration of 7 ng/μl for 48 hrs. Upon withdrawal of cisplatin, the residual cells underwent discernible morphological alterations and remained non-proliferative for an extended duration. Eventually, these cells reverted to their initial morphology and commenced regrowth (Fig. 1A, B). Dormant cancer cells, as defined by their non-proliferative state, were validated through cell cycle analysis, showing arrest in the G0/G1 phase. Reactivated cancer cells demonstrated a re-entry into the S phase (Fig. 1C, D). Importantly, this indicated dormancy rather than other non-proliferative states, specifically excluding senescence.

To comprehensively explore transcriptional profiles, we employed PacBio iso-seq for full-length cDNA sequencing. Using MatchAnnot, we compared transcript isoforms with known transcript isoforms, revealing 29,593, 21,085 and 22,314 known transcript isoforms in non-cancerous controls (NC), dormant, and reactivated cancer cells, respectively. Additionally, 455, 311 and 304 novel transcripts were identified in NC, dormant and reactivated cancer cells, respectively (Fig. 1E). The lengths of the three groups of full-length transcripts ranged from 1–10 K, mainly distributed around 2.5 K (Fig. 1F). Functional annotation, performed using NT, NR, Swissprot, KEGG and KOG/COG, detected 10,584, 7767, 8396 annotated genes across all 4 databases in NC, dormant cancer cells, and reactivated cancer cells, respectively (Fig. 1G). These findings collectively suggest that cancer cells undergo a reduction in gene

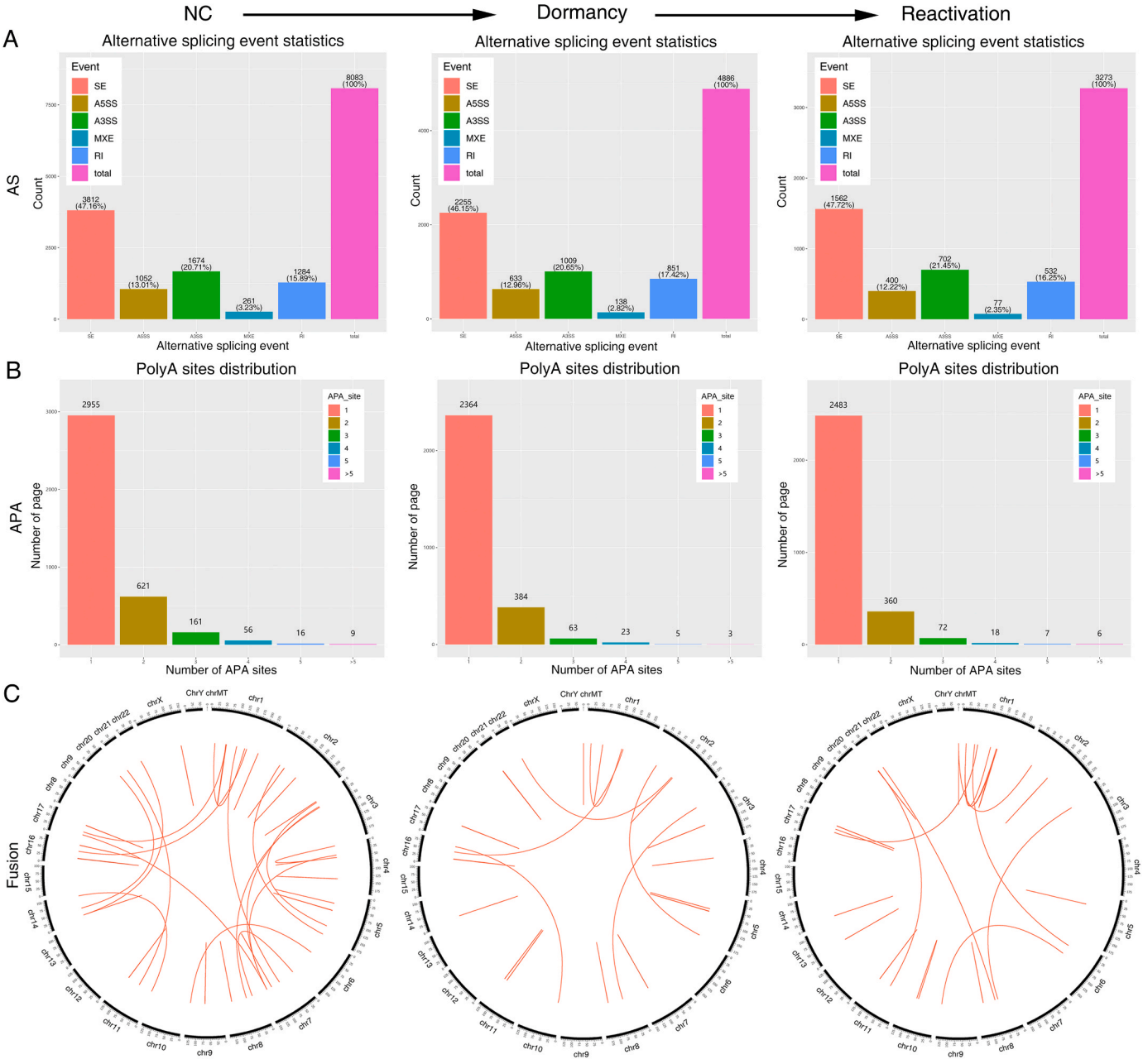

Fig. 2. Chemotherapy-responsive cancer cells displayed reduced isoform diversity. (A) Alternative splicing events, (B)APA and (C) Fusion genes in NC, dormant and reactivated cancer cells respectively.

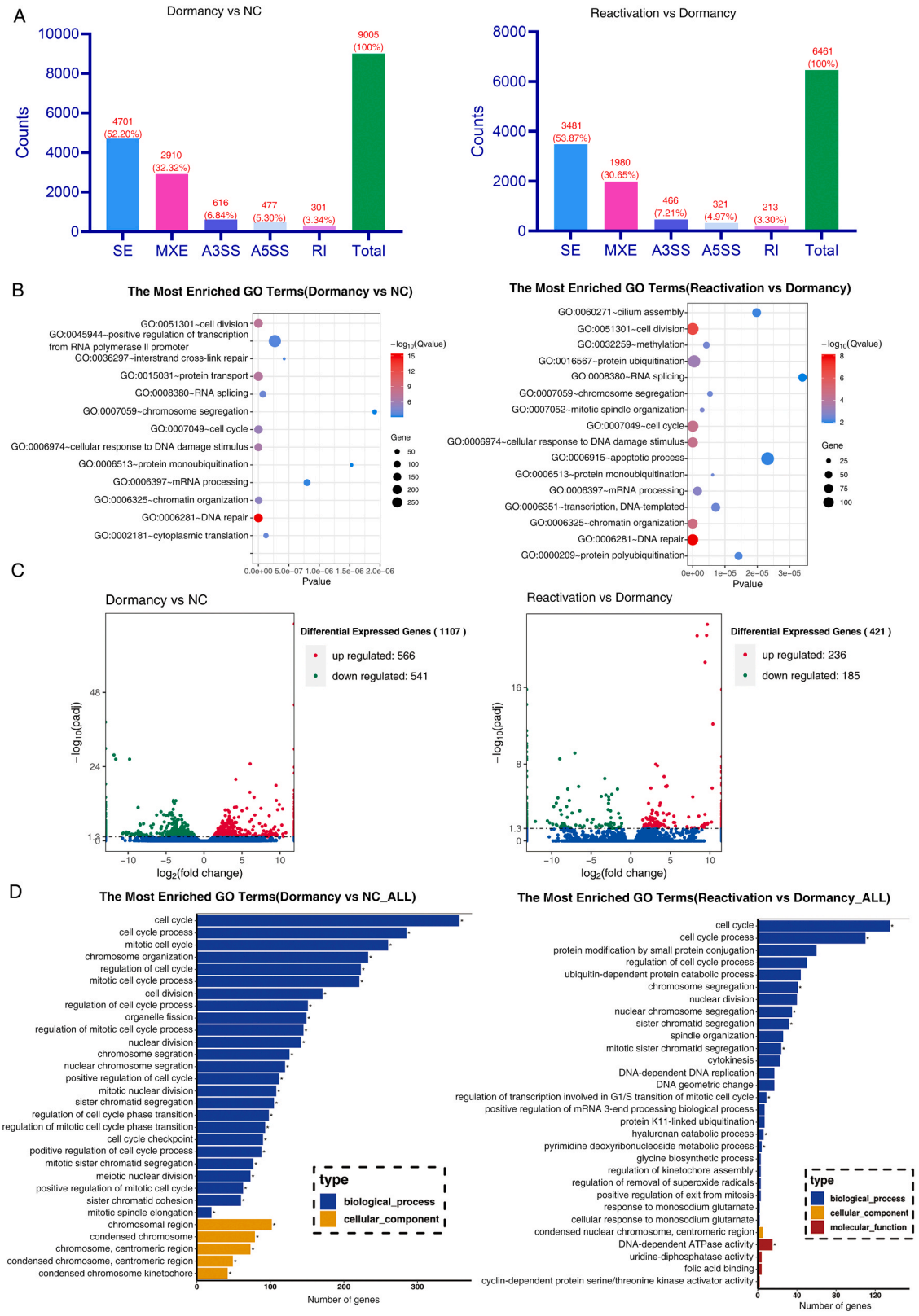

Fig. 3. Differential alternative splicing events and gene expression profiles in cisplatin-induced dormant and reactivated lung cancer cells. (A) DSEs between dormant cancer cells and normal control (NC) cells (left); DSEs between reactivated cancer cells and dormant cancer cells (right); (B) GO analysis of the DSEs between dormant cancer cells and normal control (NC) cells (left). GO analysis of DSEs among re-activated and inactive cancer cells (right); (C) DEGs between dormant cancer cells and normal control (NC) cells (left); DEGs among re-activated and inactive cancer cells (right); (D) GO analysis of the DEGs between dormant cancer cells and normal control (NC) cells (left). GO analysis of the DEGs between re-activated and dormancy cancer cells (right).

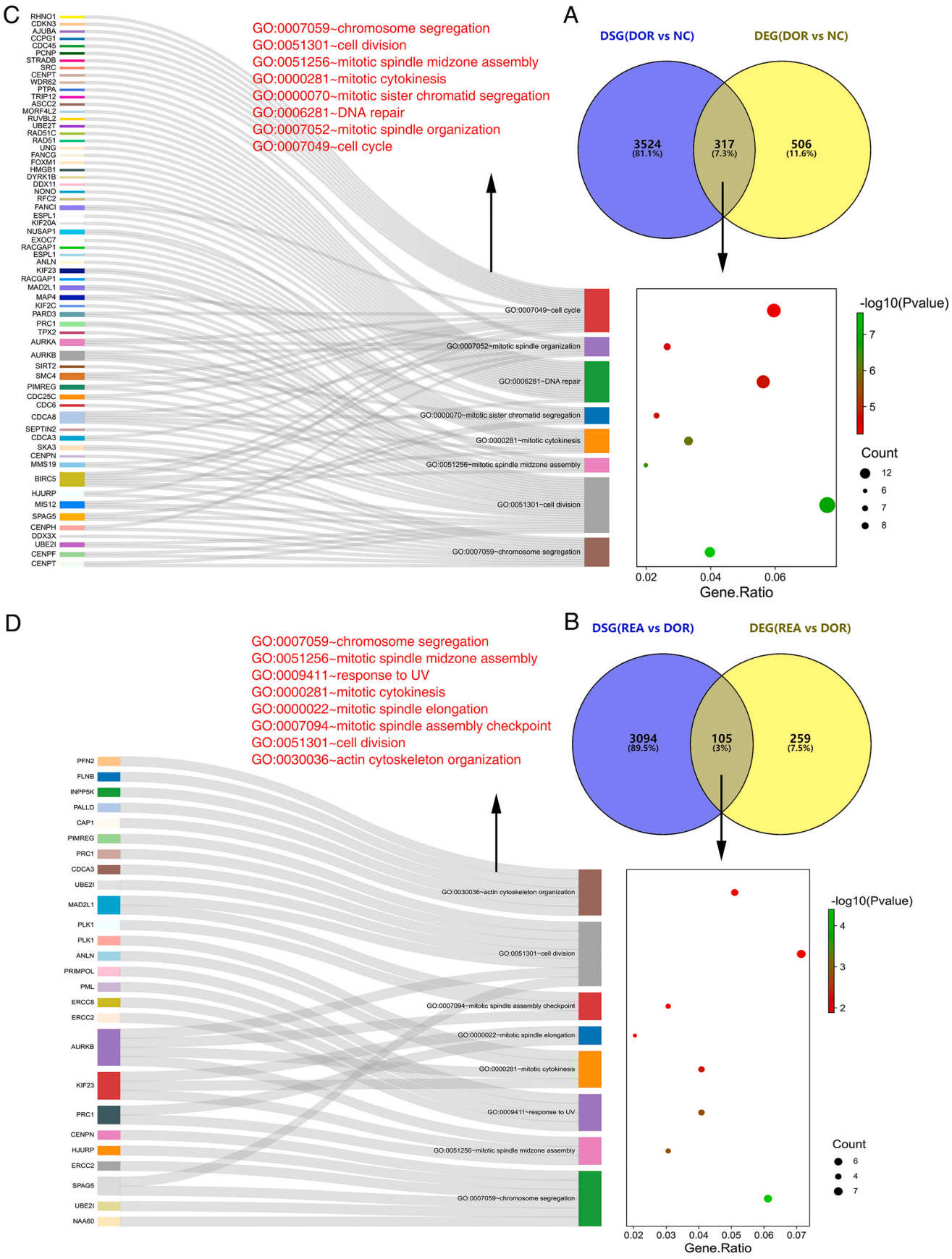

Fig. 4. Identification of overlapping DSEs and DEGs in cisplatin-induced lung cancer cells. (A) overlapping DSEs and DEGs during cellular dormancy; (B) overlapping DSEs and DEGs during cellular reactivation; GO analysis of the overlapping DSEs and DEGs between dormant cancer cells and normal control (C) and between reactivated cancer cells and dormant cancer cells (D).

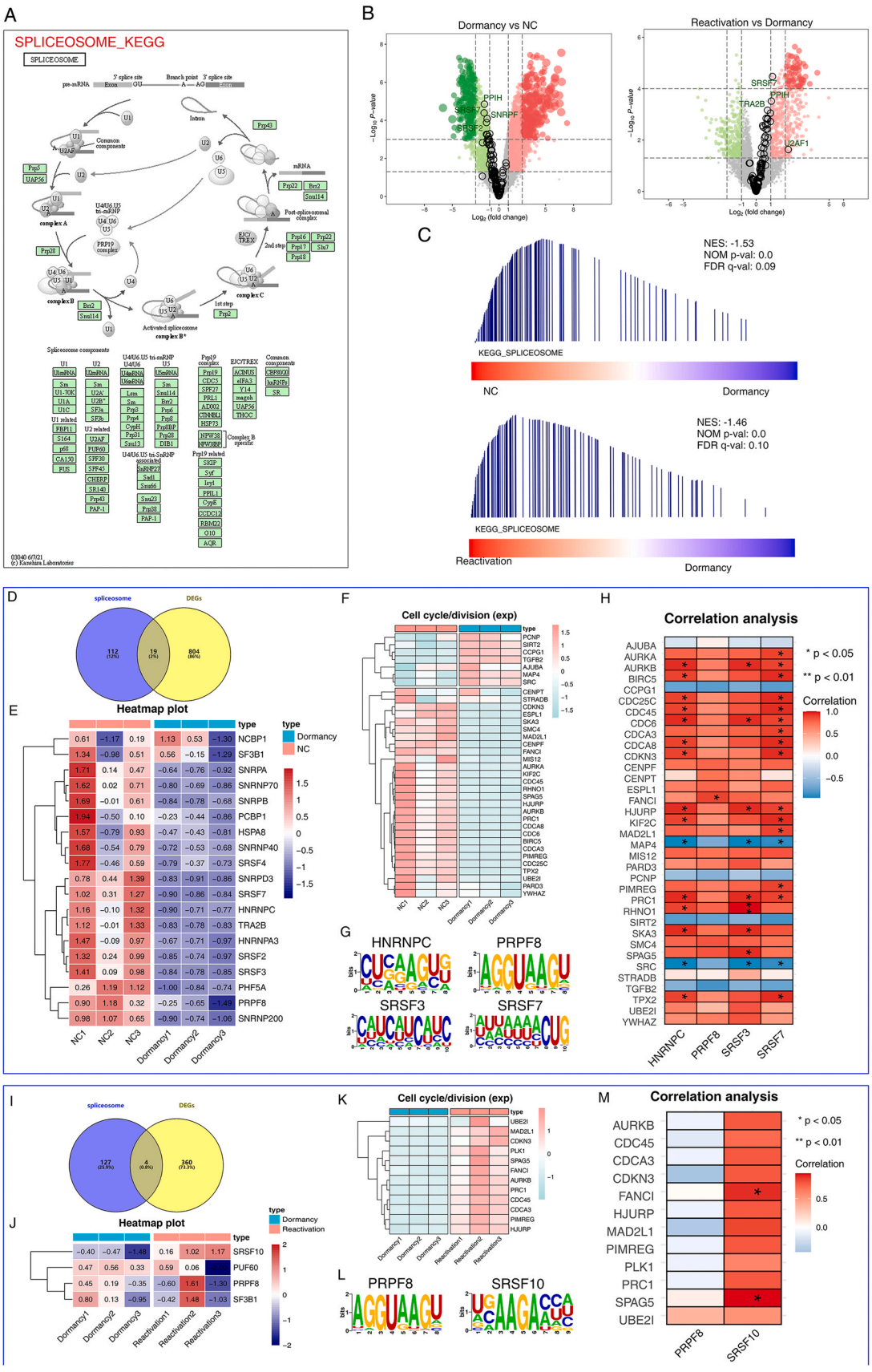

(caption on next page)

Fig. 5. Splicing factors mediates gene expression and regulates the cellular response to cisplatin. (A) Spliceosome diagram; (B) Differentially expressed splicing factors between dormant cancer cells and normal control (NC) cells (left); between reactivated cancer cells and dormant cancer cells (right); a fold change> 2 and $p < 0.05$; Red dots indicate the upregulated splicing factors and green dots indicate the downregulated splicing factors; (C) GSEA analysis of the expression of spliceosome; (D) Venn diagram showing numbers of differentially expressed genes (DEG) in spliceosome-related genes, Dormancy vs NC; (E) Heatmap of expression profile of splicing factors in dormant cancer cells; The numbers in the square indicate the relative expression values; (F,G) The heatmap of expression profile of cell cycle/cell division-related genes (upper); The splicing factor-binding motif in cell cycle/cell division-related genes (lower); (H) Correlation analysis of expression of cell cycle/cell division-related genes and splicing factors. *$P < 0.05$; (I) Venn diagram showing numbers of differentially expressed genes (DEG) in spliceosome-related genes, Reactivated vs Dormancy; (J) Heatmap of expression profile of splicing factors in reactivated cancer cells; The numbers in the square indicate the relative expression values; (K,L) The heatmap of expression profile of cell cycle/cell division-related genes (upper); The splicing factor-binding motif in cell cycle/cell division-related genes (lower); (M) Correlation analysis of expression of cell cycle/cell division-related genes and splicing factors. *$P < 0.05$. (For interpretation of the references to color in this figure legend, the reader is referred to the web version of this article.)

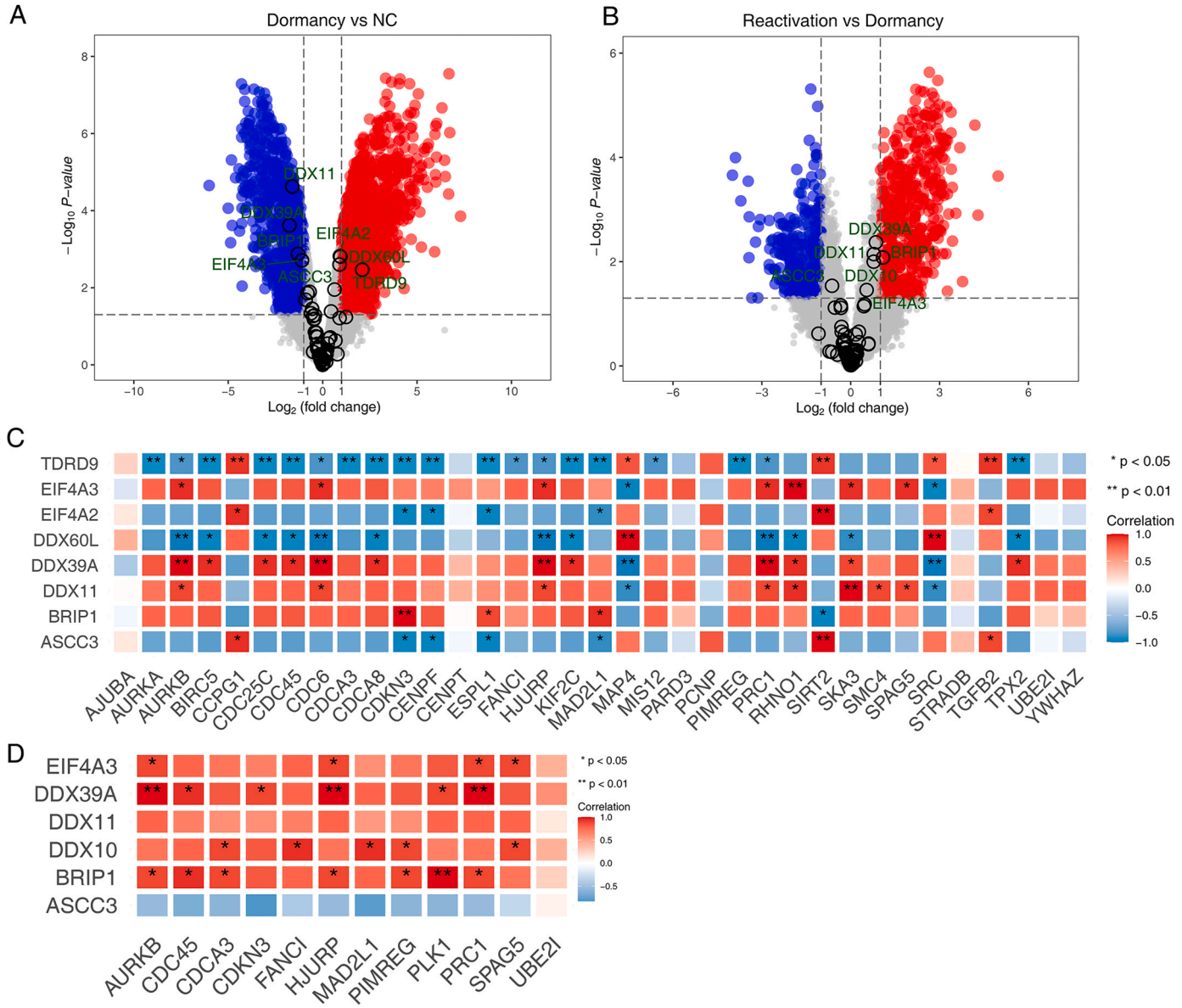

Fig. 6. The second structure of RNA affects AS. (A)(B) Volcano plot of differentially expressed RNA helicases. Red dots indicate the upregulated genes and green dots indicates the downregulated genes. Correlation analysis of expression of cell cycle/cell division-related genes and helicases between dormant cancer cells and normal control cells (C); between reactivated cancer cells and dormant cancer cells (D). *$P < 0.05$. (For interpretation of the references to color in this figure legend, the reader is referred to the web version of this article.)

transcripts in response to chemotherapeutic stress.

3.2. Chemotherapy-responsive cancer cells exhibit reduced AS events

In line with the observed reduction in gene transcripts, our investigation revealed a diminished diversity in isoforms, including alternative splicing (AS), APA, and fusion genes, in lung cancer cells undergoing cisplatin-induced dormancy and subsequent reactivation (Fig. 2A-C). To compare the alternative splicing profiles of untreated A549 cells with those of dormant and reactivated cancer cells, we used Astalavista to identify various types of alternative splicing and TAPIS pipeline (Transcriptome Analysis Pipeline for Isoform Sequencing) to predict splice

isoforms. Our results demonstrated a decrease in the majority of alternative splicing events, encompassing exon skipping, alternative 5′ or 3′ splice site selection, intron retention, and mutually exclusive exon, in dormant and reactivated cancer cells compared to untreated control cells (Fig. 2A). Additionally, Iso-seq analysis indicated 8083, 4886 and 3273 alternative splicing events in untreated negative control cells, dormant lung cancer cells and reactivated lung cancer cells, respectively (Fig. 2A). Exon skipping emerged as the most common AS event across all three groups, followed by A3, while MX was identified as the least common AS event (Fig. 2A).

3.3. Differential alternative splicing events and gene expression profiles in cisplatin-induced dormant and reactivated lung cancer cells

To explore the differential alternative splicing events (DSEs) in cisplatin-induced dormant and reactivated lung cancer cells, we identified differentially spliced genes (DSGs) using the criteria $|\Delta IncLevel| > 0.05$ and $p < 0.05$. In comparison to normal control (NC) cells, dormant cancer cells exhibited 9005 DSEs, while reactivated cancer cells showed 6461 DSEs compared to dormant cancer cells. These AS events included skipped exons (SE), retained introns (RI), alternative 3′ splice sites (A3SS), alternative 5′ splice sites (A5SS), and mutually exclusive exon (MXE) (Fig. 3A). These DSEs were primarily enriched in biological processes such as cell division, cell cycle and DNA repair (Fig. 3B).

To obtain a highly accurate genome assembly and gene expression profiles, we used both Illumina and PacBio RNA-seq data. The reads from Illumina RNA-seq were aligned to de novo transcriptome assemblies generated from PacBio sequencing using Expectation Maximization (RSEM). Subsequently, primer reads and adaptor sequencing were removed. Applying the criteria $|log2FC= \geq 1$ and q-value < 0.05, we identified 1107 (NC vs Dormancy) and 421 (Dormancy vs Relapse) DEGs, illustrated in Fig. 3C. Consistent with the functional annotation of DSGs, the DEGs were also found to be enriched in biological processes such as cell division and cell cycle (Fig. 3D).

3.4. Identification of overlapping DSEs and DEGs in cisplatin-induced lung cancer cells

We then investigated whether genes exhibiting differential mRNA expression concurrently undergo overlapping AS events. Our analysis revealed 317 and 105 overlapping events during cellular dormancy and reactivation, respectively (Fig. 4A, B). The functional annotation of these genes were enriched in biological processes such as cell cycle process, cell division and DNA repair (Fig. 4D, E). These findings imply that AS is an essential molecular mechanism orchestrating the cellular response to cisplatin.

3.5. Splicing factors mediate gene expression and govern cellular response to cisplatin

Alternative splicing events are primarily regulated by splicing factors, which can bind to cis-regulatory elements within introns and exons to regulate splicing processes (Fig. 5A). In this study, we investigated how alternative splicing events are regulated by splicing factors that bind to cis-regulatory elements in introns and exons to control splicing. Initially, we analyzed the expression profiles of these splicing factors and identified differentially expressed splicing factors using criteria of fold change> 2 and $p < 0.05$ (Fig. 5B). Gene Set Enrichment Analysis (GSEA) illustrated a downregulation of spliceosome expression in dormant cancer cells, contrasting with its reversed expression in reactivated cancer cells (Fig. 5C). Our analysis further revealed that 19 splicing factors, including hnRNPs and SRSFs, were significantly downregulated in cisplatin-induced dormant cancer cells, indicative of a reduction in alternative splicing events in these cells (Fig. 5D). Using ENCORI database, we predicted the binding affinity of splicing factors to cell cycle-related genes. Splicing factors such as SRSF7, SRSF3, PRPF8, and HNRNPC exhibited a binding affinity to cell-cycle-related genes, showing a positive correlation with their expression levels (Fig. 5E, F). Conversely, in reactivated cancer cells, the expression of splicing factors PRPF8 and SRSF10 increased, showing a positive correlation with cell-cycle-related genes (Fig. 5G-I). These findings demonstrate the pivotal role of the spliceosome in mediating gene expression and regulates the cellular response to cisplatin.

3.6. RNA secondary structure affects AS

RNA helicases, pivotal enzymes facilitating the unwinding of RNA secondary structures, play an important role in regulating alternative splicing. In our study, we investigated the roles of RNA helicases, notably DDX, EIF4A, in the cellular response of lung cancer cell to cisplatin. Our results showed significant changes in the expression of RNA helicases during cisplatin-induced dormancy and reactivation (Fig. 6A). Moreover, we observed a positive correlation between the expression of RNA helicases, such as EIF4A3, DDX39A, DDX11, BRIP1, and genes associated with cell cycle/cell division (Fig. 6B). These findings suggest the intricate relationship between RNA secondary structure, gene expression, and the regulatory role it plays in the cellular response to cisplatin.

4. Discussion

In this study, we employed a dual-sequencing approach to conduct a whole-transcriptome analysis of chemotherapy-induced lung cancer cells in both dormant and relapse states. Our findings indicate a significant reduction in gene transcripts and alternative splicing events in cisplatin-induced dormant and reactivated cancer cells. Correlation analyses revealed that splicing factors and RNA helicases orchestrated these events in response to chemotherapeutic stress.

Tumor dormancy comprises two facets: tumor mass dormancy, marked by opposing mechanisms of active cell proliferation and apoptosis, and tumor cell dormancy, characterized by inactive tumor cells in prolonged G0/G1 cell-cycle arrest [23,24]. Dormant cancer cells are considered to be responsible for tumor recurrence and treatment failure [25], In this study, we employed a cell model simulating sequential dormancy and reactivation after chemotherapy, revealing a process of sequential epithelial-mesenchymal transition (EMT) to mesenchymal-epithelial transition (MET) with enrichment of cancer stem cells. Reactivated cancer cells exhibited more aggressiveness and therapy resistance [10]. To understand these processes at the molecular level, we performed a combined transcriptome analysis using RNA-seq and SMRT sequencing. By integrating Illumina and PacBio sequencing data, we achieved highly contiguous assemblies with improved accuracy and completeness. The third-generation sequencing technology, utilizing single-molecule real-time (SMRT) sequencing, generates long reads spanning entire transcripts without the need for fragmentation or assembly. While RNA-seq produces short reads, compromising the accuracy of assembly and annotation, SMRT sequencing, producing full-length transcripts, significantly enhances sequencing result accuracy [26,27]. The availability of SMRT sequencing technology on the PacBio platform facilitates the de novo assembly of eukaryotic transcriptomes [28]. On the other hand, SMRT sequencing still faces limitations in precisely elucidating transcript expression. The combined Illumina and PacBio data enable the generation of highly contiguous assemblies, improving accuracy and completeness. The third-generation sequencing technology generates read length in the scale of kilobase pairs, which results in improved assembly, cartographic certainty, transcript isoform recognition and structural variation detection [29].

Alternative splicing, a complex process regulated by pre-mRNA sequence, the spliceosome, and RNA-binding proteins, has been implicated in a variety of diseases, including cancer and neurological disorders. Dysregulation of alternative splicing contributes to tumorigenesis by promoting cancer cell proliferation, migration, and survival. In cancer cells, dysregulated alternative splicing leads to the production of

aberrant protein isoforms that drive tumor growth and metastasis. Following chemotherapy, a downregulation of overall alternative splicing events was observed, suggesting potential inhibition of the spliceosome pathway [30]. Recent studies suggest that cancer cells can strategically downregulate gene expression by diminished alternative splicing events, mediated by splicing factors and RNA helicases, in response to chemotherapeutic stress [31]. This adaptive mechanism is believed to confer an advantage to cancer cells by promoting cancer cell survival and resistance to chemotherapy [31].

The regulation of alternative splicing involves a sophisticated interplay between splicing factors and RNA helicases, dictating the splicing outcomes by finely tuning the balance between exon inclusion and exclusion. RNA helicases, pivotal enzymes in RNA metabolism, unwind RNA secondary structures and facilitate RNA-protein interactions. Belonging to the class of motor proteins, RNA helicases participate in diverse aspects of RNA metabolism, including transcription, translation, RNA processing, and RNA decay. In this study, we observed a reduction in gene transcripts and alternative splicing events in cisplatin-induced dormant and reactivated lung cancer cells. The intersection of differentially expressed genes and differentially spliced genes revealed enrichment in the cell cycle and cell division pathways. This implies that alternative splicing is a key mechanism mediating the cellular response to chemotherapy. In this study, the observed inhibition of alternative splicing following chemotherapy may represent a survival strategy employed by cancer cells to adapt to the cytotoxic effects of the treatment. Further experimental validation is needed to elucidate the specific splicing events and molecules involved in mediating these adaptive responses in cancer cells.

Splicing factors and RNA helicases play important roles in regulating the splicing process. They can act at multiple steps in the splicing pathway, including the assembly of the spliceosome, recognition of splice sites, and the release of the mature mRNA product. RNA helicases exhibit interaction with both the pre-mRNA substrate and the spliceosome complex, influencing splicing efficiency, specificity, and regulation. Chemotherapy can directly target RNA helicases, leading to their inhibition or degradation. While the study highlights the involvement of splicing factors and RNA helicases in the alternative splicing events, the precise mechanistic details of how these factors orchestrate the procell remain partially elucidated.

In conclusion, our findings indicate that lung cancer cells respond to chemotherapeutic stress by diminishing gene transcripts through reduced alternative splicing events, a process mediated by splicing factors and RNA helicases. These findings provide valuable information regarding the molecular mechanisms implicated in the therapeutic selection and reactivation of dormant cancer cells. Furthermore, this comprehension unveils potential avenues for developing therapeutic strategies aimed at preventing cancer recurrence post-chemotherapy. Nonetheless, further research is needed to comprehensively validate and understand these mechanisms.

Ethics approval and consent to participate

Not applicable.

Consent for publication

All authors have read and approved the manuscript.

Funding

This work was supported by National Natural Science Foundation, China (grant number 81773147, 81972198); the Natural Science Foundation of Hunan Province (grant number 2023JJ40853); Natural Science Foundation, Changsha (grant number kq2208299, kq2208337); Strategic Priority Research Program of Central South University (ZLXD2017004).

CRediT authorship contribution statement

Lu-juan Wang: Conceptualization, Software, Data curation, Writing – original draft, Visualization, Software, Funding acquisition. **Na Yin:** Data curation, Methodology, performed the experiments. **Wen-hua Shi:** Software, Validation. **Yao-huan Xie:** Data curation, Software. **Jun-qi Yi:** Data curation, Software. **Zi-ying Tang:** Data curation, Software. **Jing-qun Tang:** Conceptualization, Methodology, Software, Visualization, Investigation, Supervision, Funding acquisition. **Juan-juan Xiang:** Conceptualization, Visualization, Investigation, Supervision, Writing – review & editing, Funding acquisition.

Declaration of Competing Interest

The authors declare that they have no known competing financial interests or personal relationships that could have appeared to influence the work reported in this paper.

Data availability

The datasets generated and analyzed in the current study are available in the Sequence Read Archive (SRA) database at NCBI under BioProject ID PRJNA730205 and PRJNA793575.

Acknowledgements

Not applicable.

Appendix A. Supporting information

Supplementary data associated with this article can be found in the online version at doi:10.1016/j.csbj.2023.12.039.

References

[1] Chen SH, Chang JY. New insights into mechanisms of cisplatin resistance: from tumor cell to microenvironment. Int J Mol Sci 2019;20(17).
[2] Endo H, Inoue M. Dormancy in cancer. Cancer Sci 2019;110(2):474–80.
[3] Giancotti FG. Mechanisms governing metastatic dormancy and reactivation. Cell 2013;155(4):750–64.
[4] Walens A, Lin J, Damrauer JS, McKinney B, Lupo R, Newcomb R, et al. Adaptation and selection shape clonal evolution of tumors during residual disease and recurrence. Nat Commun 2020;11(1):5017.
[5] Ule J, Blencowe BJ. Alternative splicing regulatory networks: functions, mechanisms, and evolution. Mol Cell 2019;76(2):329–45.
[6] Wang B, Kumar V, Olson A, Ware D. Reviving the transcriptome studies: an insight into the emergence of single-molecule transcriptome sequencing. Front Genet 2019;10:384.
[7] Wu Q, Wang J, Mao S, Xu H, Wu Q, Liang M, et al. Comparative transcriptome analyses of genes involved in sulforaphane metabolism at different treatment in Chinese kale using full-length transcriptome sequencing. BMC Genom 2019;20(1):377.
[8] Zhang D, Li W, Chen ZJ, Wei FG, Liu YL, Gao LZ. SMRT- and Illumina-based RNA-seq analyses unveil the ginsinoside biosynthesis and transcriptomic complexity in Panax notoginseng. Sci Rep 2020;10(1):15310.
[9] Xiao R, Chen JY, Liang Z, Luo D, Chen G, Lu ZJ, et al. Pervasive chromatin-RNA binding protein interactions enable RNA-based regulation of transcription. Cell 2019;178(1):107–21. e118.
[10] Wang L, Peng Q, Xie Y, Yin N, Xu J, Chen A, et al. Cell-cell contact-driven EphB1 cis- and trans- signalings regulate cancer stem cells enrichment after chemotherapy. Cell Death Dis 2022;13(11):980.
[11] Li R, Li Y, Kristiansen K, Wang J. SOAP: short oligonucleotide alignment program. Bioinformatics 2008;24(5):713–4.
[12] Kim D, Langmead B, Salzberg SL. HISAT: a fast spliced aligner with low memory requirements. Nat Methods 2015;12(4):357–60.
[13] Babarinde IA, Li Y, Hutchins AP. Computational methods for mapping, assembly and quantification for coding and non-coding transcripts. Comput Struct Biotechnol J 2019;17:628–37.
[14] Langmead B, Salzberg SL. Fast gapped-read alignment with Bowtie 2. Nat Methods 2012;9(4):357–9.
[15] Li B, Dewey CN. RSEM: accurate transcript quantification from RNA-Seq data with or without a reference genome. BMC Bioinform 2011;12:323.
[16] Love MI, Huber W, Anders S. Moderated estimation of fold change and dispersion for RNA-seq data with DESeq2. Genome Biol 2014;15(12):550.

[17] Foissac S, Sammeth M. ASTALAVISTA: dynamic and flexible analysis of alternative splicing events in custom gene datasets. Nucleic Acids Res 2007;35(Web Server issue):W297–9.
[18] Lian B, Hu X, Shao ZM. Unveiling novel targets of paclitaxel resistance by single molecule long-read RNA sequencing in breast cancer. Sci Rep 2019;9(1):6032.
[19] Shen S, Park JW, Lu ZX, Lin L, Henry MD, Wu YN, et al. rMATS: robust and flexible detection of differential alternative splicing from replicate RNA-Seq data. Proc Natl Acad Sci USA 2014;111(51):E5593–601.
[20] Xu J, Wang L, Yin N, Chen A, Yi J, Tang J, et al. Proteomic profiling of extracellular vesicles and particles reveals the cellular response to cisplatin in NSCLC. Thorac Cancer 2021;12(19):2601–10.
[21] Wang L, Peng Q, Yin N, Xie Y, Xu J, Chen A, et al. Chromatin accessibility regulates chemotherapy-induced dormancy and reactivation. Mol Ther Nucleic Acids 2021; 26:269–79.
[22] Li S, Kennedy M, Payne S, Kennedy K, Seewaldt VL, Pizzo SV, et al. Model of tumor dormancy/recurrence after short-term chemotherapy. PLoS One 2014;9(5): e98021.
[23] Davis Jr JE, Kirk J, Ji Y, Tang DG. Tumor dormancy and slow-cycling cancer cells. Adv Exp Med Biol 2019;1164:199–206.
[24] Aguirre-Ghiso JA. Models, mechanisms and clinical evidence for cancer dormancy. Nat Rev Cancer 2007;7(11):834–46.
[25] Sauer S, Reed DR, Ihnat M, Hurst RE, Warshawsky D, Barkan D. Innovative approaches in the battle against cancer recurrence: novel strategies to combat dormant disseminated tumor cells. Front Oncol 2021;11:659963.
[26] Zhang P, Jiang D, Wang Y, Yao X, Luo Y, Yang Z. Comparison of De Novo assembly strategies for bacterial genomes. Int J Mol Sci 2021;22(14).
[27] Roberts RJ, Carneiro MO, Schatz MC. The advantages of SMRT sequencing. Genome Biol 2013;14(7):405.
[28] Tan C, Liu H, Ren J, Ye X, Feng H, Liu Z. Single-molecule real-time sequencing facilitates the analysis of transcripts and splice isoforms of anthers in Chinese cabbage (Brassica rapa L. ssp. pekinensis). BMC Plant Biol 2019;19(1):517.
[29] Amarasinghe SL, Su S, Dong X, Zappia L, Ritchie ME, Gouil Q. Opportunities and challenges in long-read sequencing data analysis. Genome Biol 2020;21(1):30.
[30] Anufrieva KS, Shender Vcapital OC, Arapidi GP, Pavlyukov MS, Shakhparonov MI, Shnaider PV, et al. Therapy-induced stress response is associated with downregulation of pre-mRNA splicing in cancer cells. Genome Med 2018;10(1):49.
[31] Biamonti G, Caceres JF. Cellular stress and RNA splicing. Trends Biochem Sci 2009; 34(3):146–53.